Supporting Information

Efficient Electrochemical CO_2 Conversion by Cobalt-Based Metal Organic Frameworks Modified by Bimetallic Gold-Silver Nanostructures

Mohammadali Beheshti[a], Mohsen Saeidi[a], MahsaSadat Adel Rastkhiz[a], Shohreh Shahrestani[b], Ali Zarrabi[c], Jing Bai[d], Abdolreza Simchi[a,e†], Samineh Akbarmolaei[a]

[a] Department of Materials Science and Engineering, Sharif University of Technology, Tehran 1458889694, Iran

[b] Centre for Corrosion Research, Mechanical Engineering Department, Universiti Teknologi PETRONAS, Seri Iskandar 32610, Malaysia

[c] Biomedical Engineering Department, Faculty of Engineering and Natural Sciences, Istinye University, Istanbul 34396, Turkey

[d] *School of Environmental Science and Engineering, Key Laboratory of Thin Film and Microfabrication Technology (Ministry of Education), Shanghai Jiao Tong University, Shanghai200240, P. R. China*

[e] Institute for Nanoscience and Nanotechnology, Sharif University of Technology, Tehran 14588, Iran

[†] Corresponding author: Tel: +98-21-6616 5226. E-mail: Simchi@sharif.edu

List of content

S1. Materials and methods

Table S1. Materials and process parameters used for CO_2RR

Anolyte	0.1 M H_2SO_4
Counter electrode	Platinum
Reference electrode	Ag/AgCl
Working electrodes	Ag@ZIF-67/GCE, Au@ZIF-67/GCE, and Au-Ag@ZIF-67/GCE
Catholyte	0.1 M K_2CO_3
Cell type	H-Shaped
Process	Chronoamperometry (CA) @ -1 V vs. RHE De-oxidation for 30 min with N_2 gas Inlet CO_2 with a rate of 20 mL/min Temperature: 25 ºC

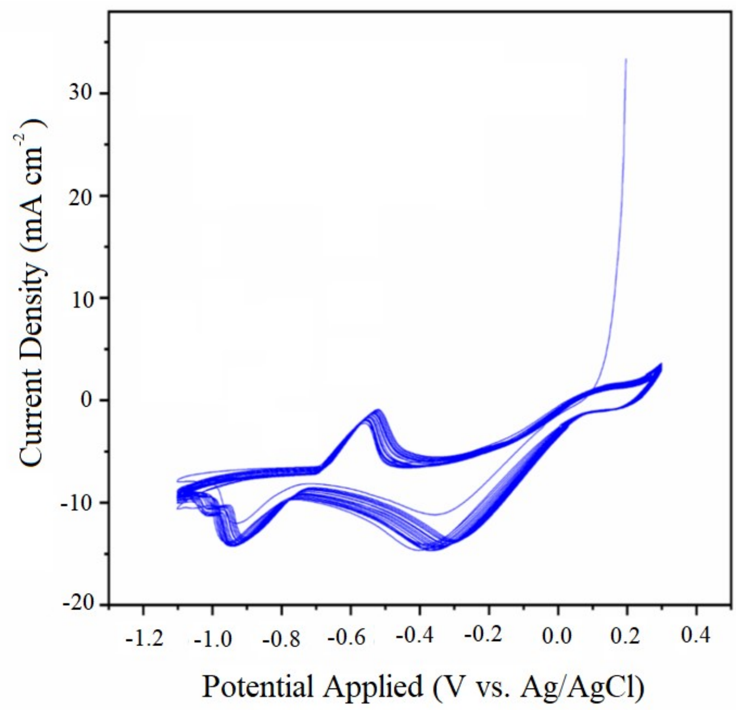

Figure S1. Cyclic voltammograms for electrodeposition of gold and silver nanoparticles on ZIF-67/GCE at a scan rate of 200 mV s^{-1} for 15 cycles.

S2. Determination of the particle size distribution of electrocatalysts

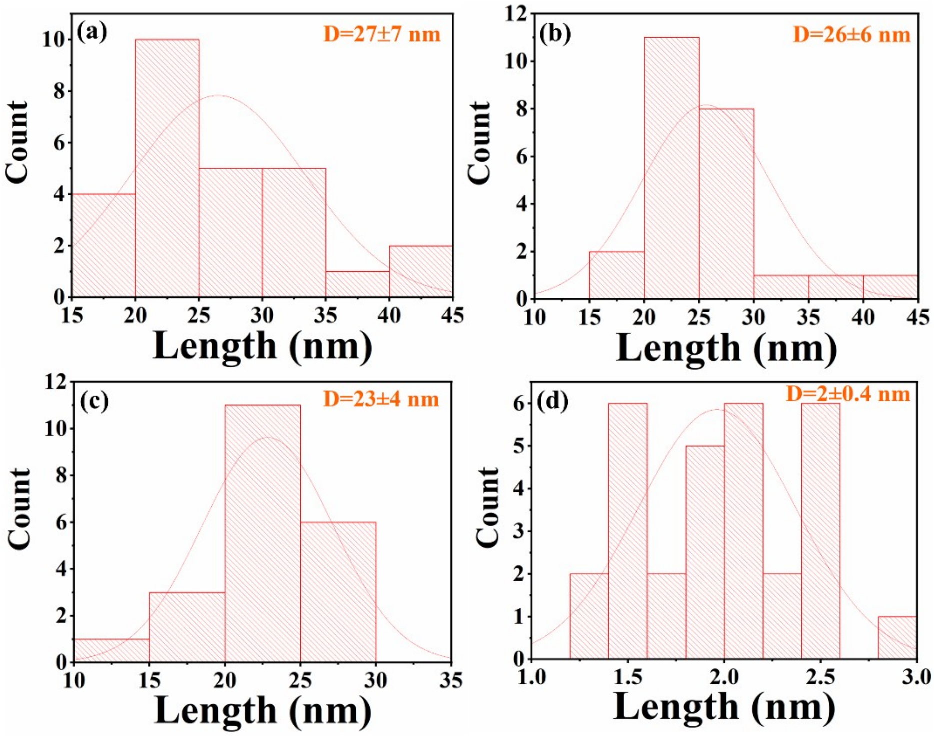

Figure S2. Particle size distribution of (a) Ag@ZIF-67, (b) Au@ZIF-67, and (c) Au-Ag@ZIF-67 electrocatalysts determined by FE-SEM. (d) Particle size distribution of Au-Ag@ZIF-67 determined by HRTEM.

S3. TEM and EDS analyses

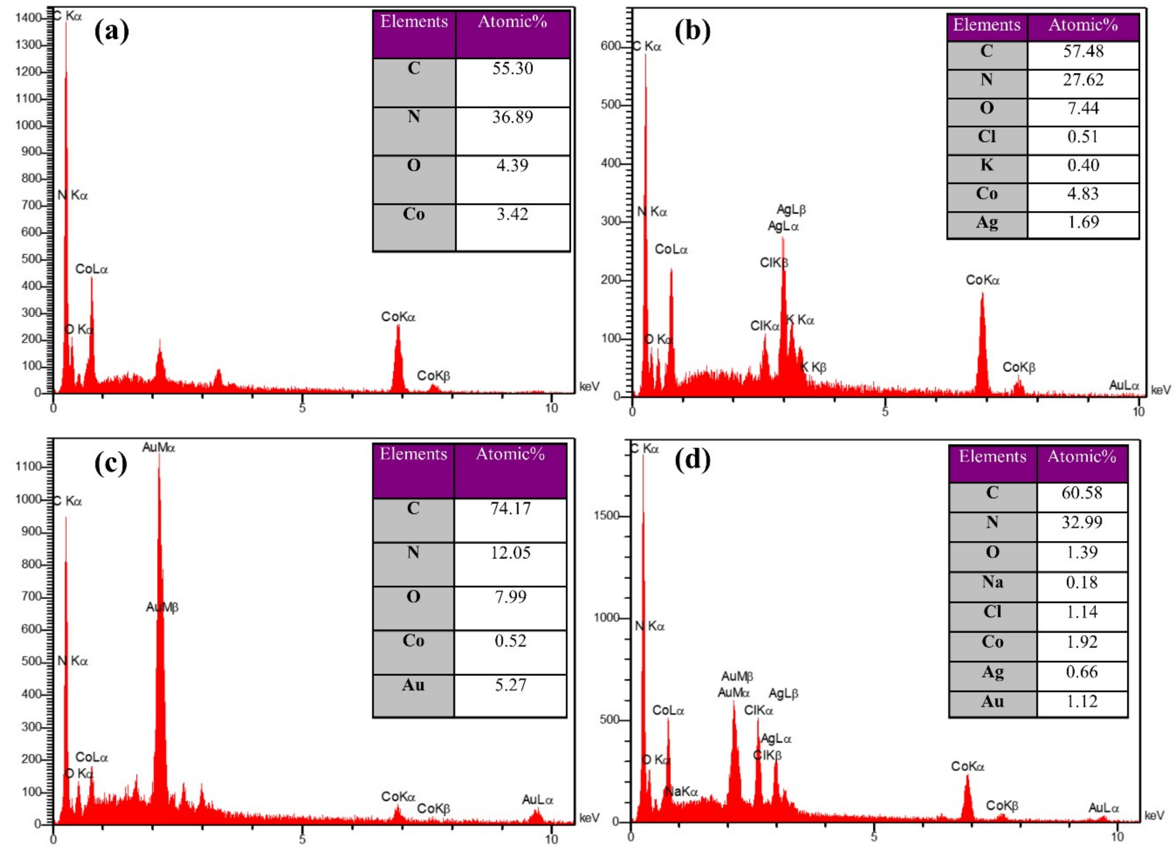

Figure S3. EDS spectra of (a) ZIF-67, (b) Ag@ZIF-67, (c) Au@ZIF-67 and (d) Au-Ag@ZIF-67.

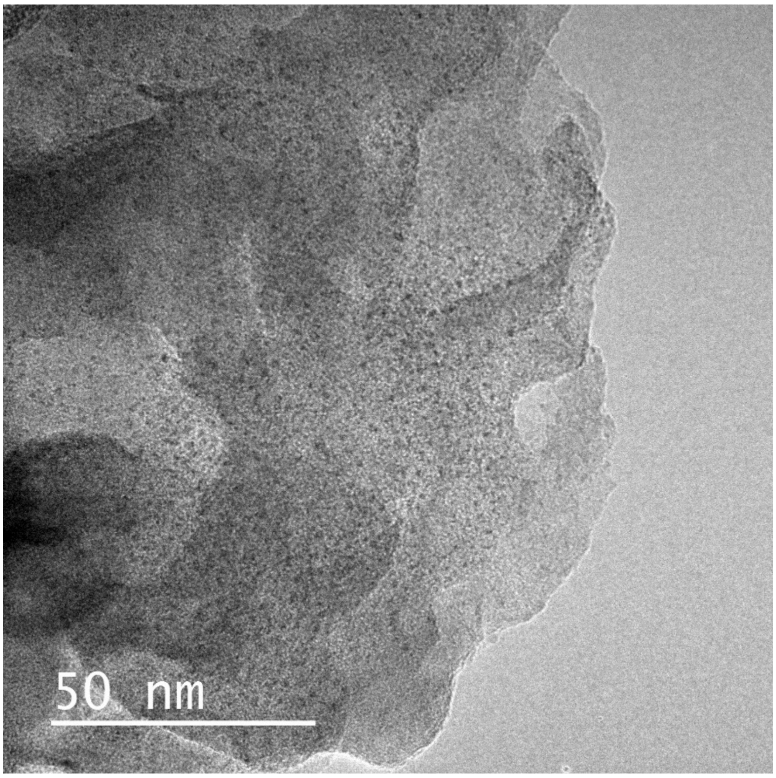

Figure S4. TEM image of Au-Ag@ZIF-67.

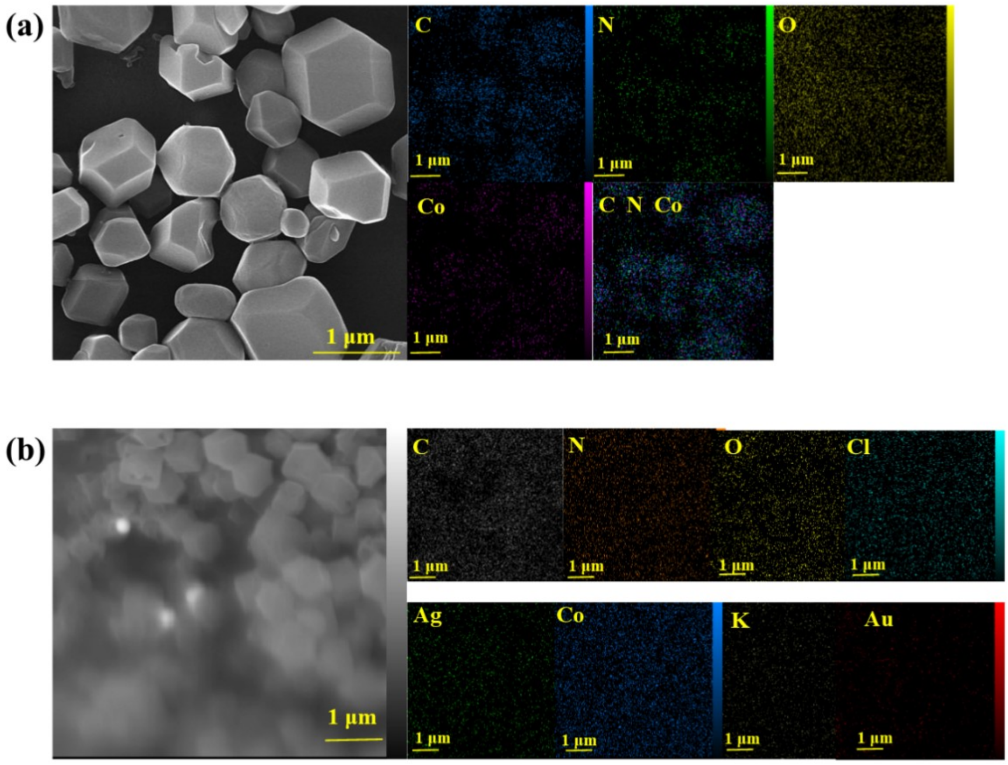

Figure S5. EDS mapping of (a) ZIF-67 and (b) Au-Ag@ZIF-67.

S.4 XPS analysis

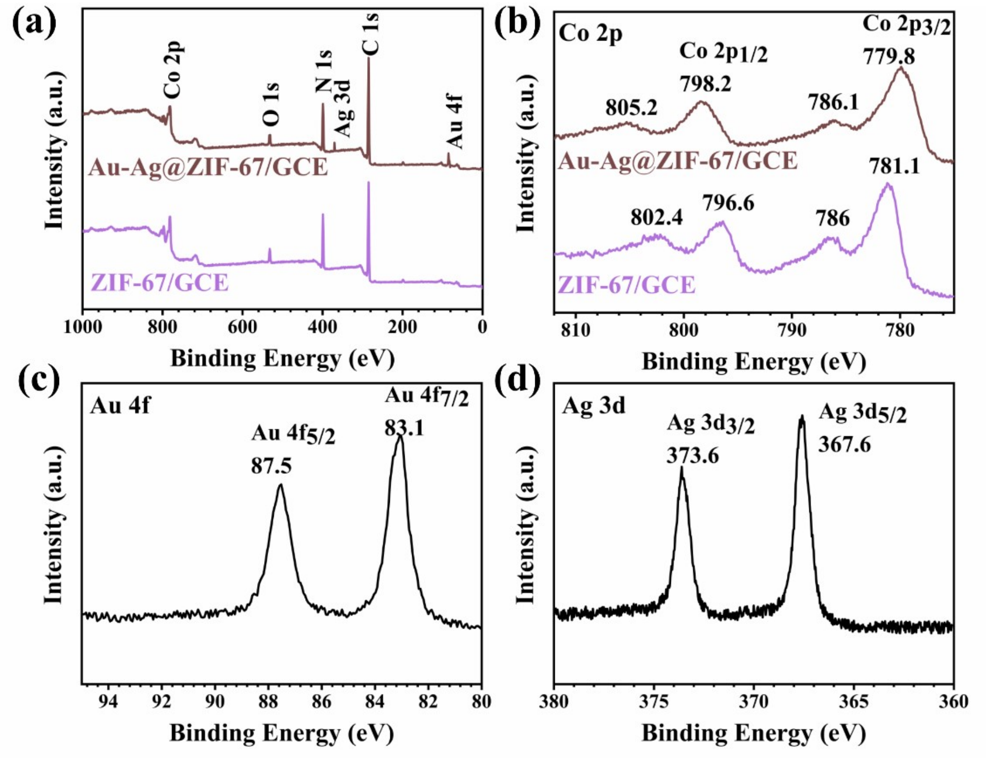

Figure S6. XPS spectra of (a)ZIF-67/GCE and Au-Ag@ ZIF-67/GCE, (b) Co 2p, (c) Au 4f and (d) Ag 3d.

S5. Electrochemical studies

Table S2. Values of R_s and R_{ct} derived from ESI data fitting by an equivalent circuit

Substrate	R_s (Ω)	R_{ct} (Ω)
GCE	32. 4	193.3
ZIF-67/GCE	41.9	266.1
Ag/GCE	32.8	143.7
Au/GCE	38.6	16.4
Au-Ag/GCE	33.2	35.1
Ag@ZIF-67/GCE	22.4	189.3
Au@ZIF-67/GCE	22.9	1.5
Au-Ag@ZIF-67/GCE	18.6	0.14

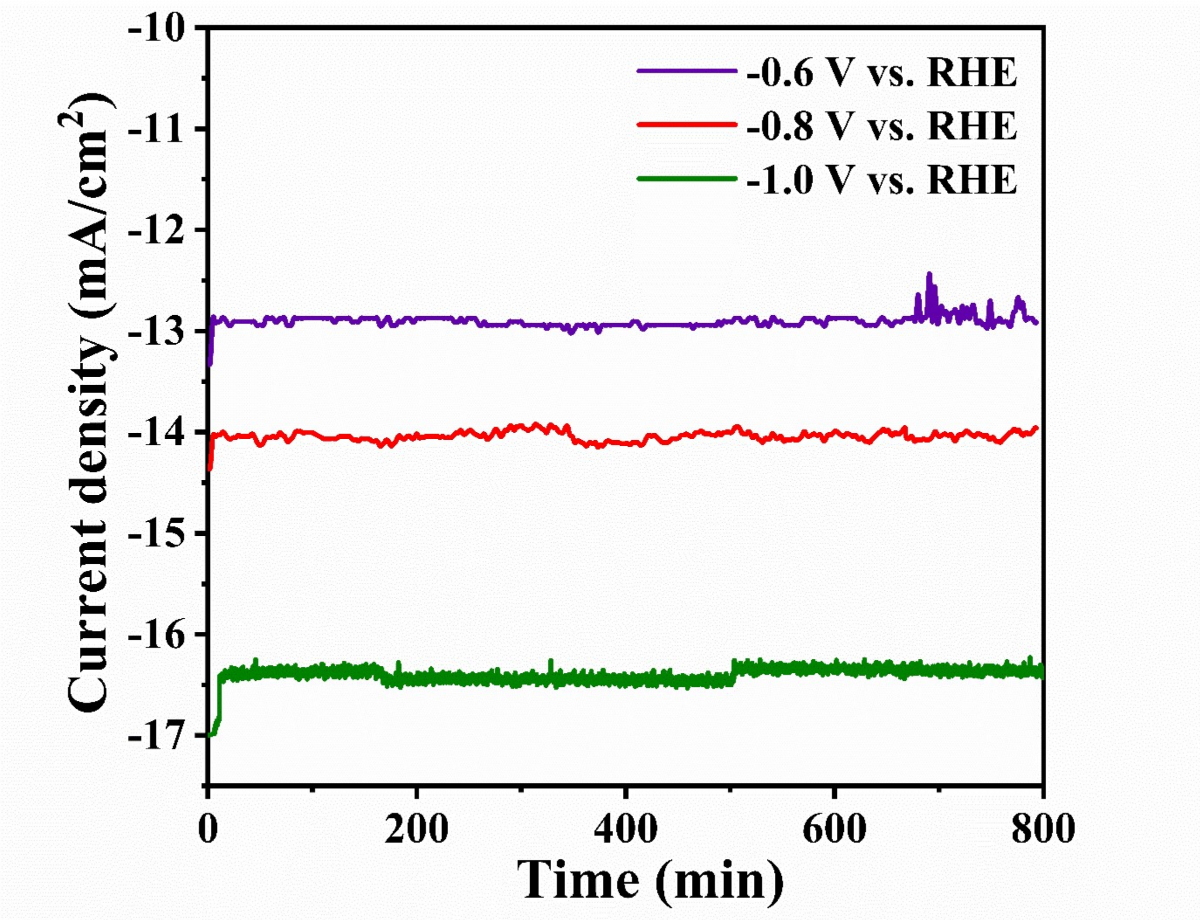

Figure S7. Amperometric studies as a function of time at the potentials of -0.6, -0.8, and -1 V (vs. RHE) showing the stability of the Au-Ag@ZIF-67 catalyst for CO_2RR

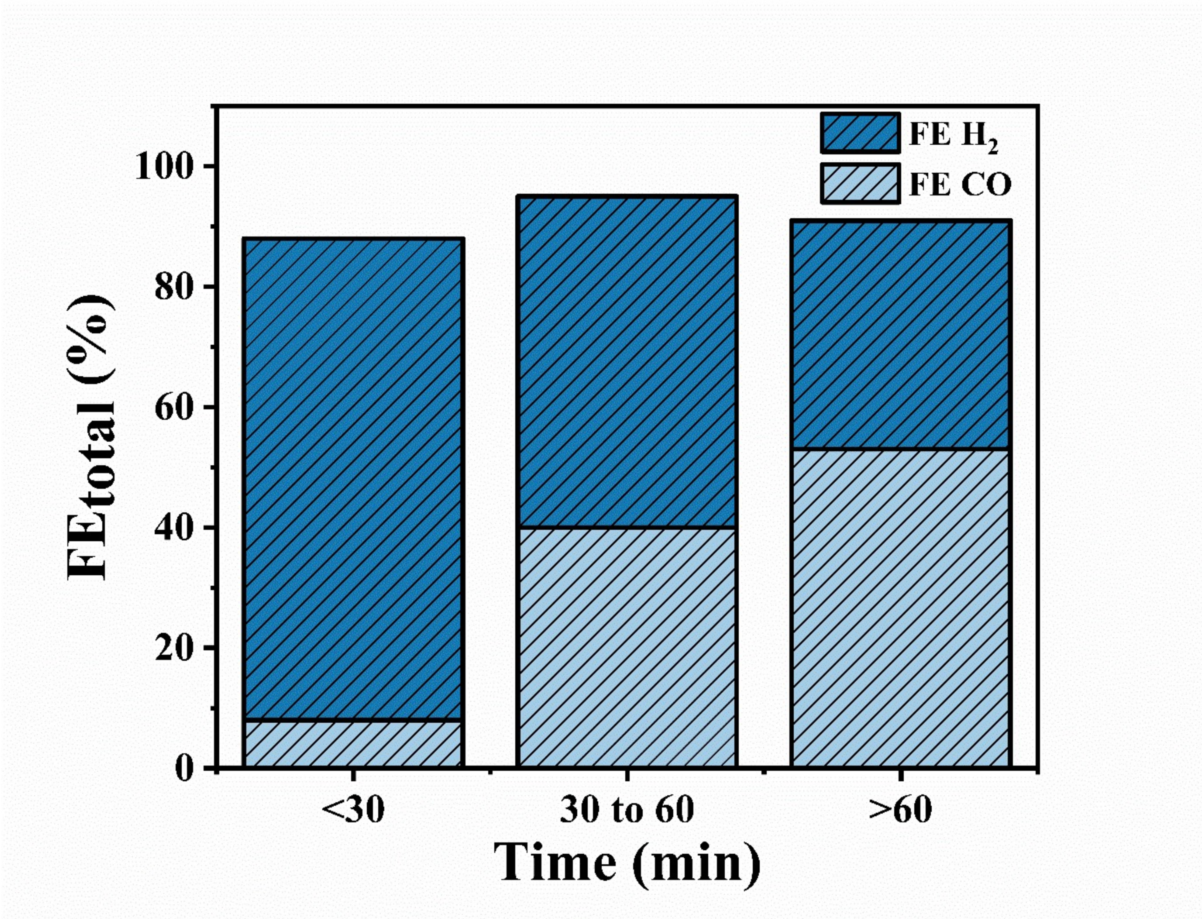

Figure S8. Time-dependent Faradaic efficiencies of gas products on the Au-Ag@ZIF-67 catalyst at -1 V (vs. RHE) for CO_2RR

S5.1. Electrochemical active surface area (ECSA)

CV at multiple scan rates was performed in a solution of 5 mM $Fe(CN)_6^{3-/4-}$ containing 0.1 M KCl to determine (ECSA). The Randles-Sevcik plot derived from CV curves is shown in Figure S5, and the value of ECSA was calculated by[1]:

$$I_p = (2.69 \times 10^5) n^{\frac{3}{2}} A D^{\frac{1}{2}} v^{\frac{1}{2}} C_0 \quad \text{(S1)}$$

where I_p is the peak current (A), n is the number of the electrons participating in the reaction, A is the surface area of the electrode (cm^2), D is the diffusion coefficient of the electroactive species ($cm^2\ s^{-1}$), v is the scan reate ($V\ s^{-1}$), and C_0 is the concentration of the electroactive species in the bulk solution. Based on the slope of I_p vs. $v^{1/2}$, the ECSA was calculated for each electrode and shown in Table S3.

Table S3. The calculated values of ECSA

Substrate	Slope	Electroactive area (cm^2)
GCE	0.19	0.054
ZIF-67/GCE	0.17	0.04
Ag/GCE	0.28	0.08
Au/GCE	0.3	0.083
Au-Ag/GCE	0.26	0.074
Ag@ZIF-67/GCE	0.46	0.13
Au@ZIF-67/GCE	0.54	0.15
Au-Ag@ZIF-67/GCE	0.63	0.18

Table S4. The extracted data from LSV curves of electrochemical CO_2RR

Substrate	Overpotential at -10 mA (vs. RHE)	Current at -1 V (vs. RHE) (mA)
GCE	-	-1.54
ZIF-67/GCE	-	-0.7
Ag@ZIF-67/GCE	-0.63	-12.29
Au@ZIF-67/GCE	-0.58	-12.69
Au-Ag@ZIF-67/GCE	-0.54	-16.4

S6. Stability studies for CO_2 reduction reaction

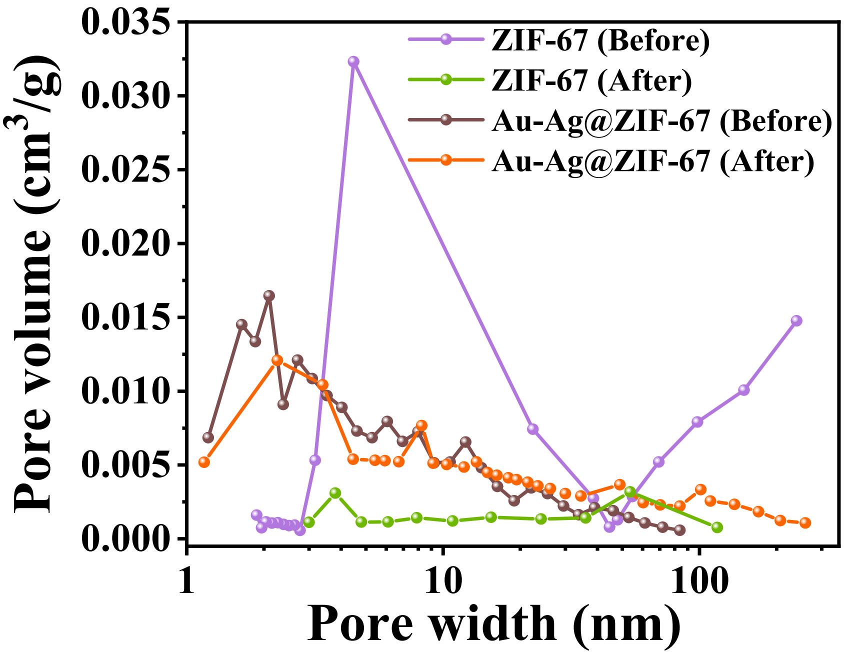

Figure S9. BJH pore size distribution.

Table S5. N_2 adsorption/desorption data for the synthesized samples

Sample	S_{BET} (m^2 g^{-1})	S_{ext} (m^2 g^{-1})	S_{micro} (m^2 g^{-1})	V_{micro} (cm^3 g^{-1})	V_{total} (cm^3 g^{-1})	Mean pore width (nm)
ZIF-67 before CO_2 reduction	1705.1	17.8	1755.7	0.613	0.667	7.2
ZIF-67 after CO_2 reduction	196.4	4.1	204.8	0 .092	0 .104	10.9
Au-Ag@ZIF-67 before CO_2 reduction	1072.5	55.6	1016.9	0.510	0.560	5.7
Au-Ag@ZIF-67 after CO_2 reduction	985.3	43.2	940.1	0.49	0.546	6.2

References

1 A. J. Bard, L. R. Faulkner and H. S. White, in *Electrochemical Methods: Fundamentals and Applications*, John Wiley & Sons, Ltd, New Jersey, 3rd edn., 2022, p. 316.